PNAS RESEARCH ARTICLE | CHEMISTRY

Unveiling street art: A multimodal and multitechnique approach for analyzing and mapping painting materials on large murals

Francesca Sabatini[a,1], Fauzia Albertin[a,2], Brenda Doherty[a], Letizia Monico[a,b], Francesca Rosi[a], David Buti[c], Aldo Romani[a,b], Antonio Pecci[a,d,3], Nicodemo Abate[d], Maria Sileo[d], Antonio Minervino Amodio[d], Nicola Masini[d], Silvia Pizzimenti[e,4], Ilaria Degano[e], Francesca Modugno[e], Beatrice Campanella[f], Stefano Legnaioli[f], and Laura Cartechini[a,5]

Affiliations are included on p. 10.

Edited by Admir Masic, Massachusetts Institute of Technology, Cambridge, MA; received March 5, 2025; accepted July 11, 2025 by Editorial Board Member Joanna Aizenberg

Street art murals are increasingly recognized as valuable contemporary artworks, often attaining significant artistic, historical, and social importance. As these murals become integral parts of cultural heritage, finding efficient strategies for their conservation is crucial. However, their typical large surface areas, heterogeneous materials, and high variability in exposure to environmental and pollution factors pose significant challenges in establishing appropriate analytical strategies to obtain the necessary information. This study proposes a multiscale and multitechnique noninvasive approach to investigate and monitor street art murals in situ. By combining portable point techniques—such as external reflection Fourier transform infrared spectroscopy, Raman spectroscopy, visible, near infrared, and short-wave infrared reflectance spectroscopy, and X-ray fluorescence spectroscopy—with visible and near infrared hyperspectral imaging, the mural's composition across a square meter surface could be analyzed. Additionally, multispectral imaging mounted on a drone provided a global reconstruction and characterization of the overall mural. This method was complemented by microdestructive laboratory analyses of selected samples, using pyrolysis gas chromatography–mass spectrometry and liquid chromatography coupled with diode array detector and tandem mass spectrometry, to further investigate selected samples and support noninvasive results. The approach was applied to the iconic mural "Musica Popolare" (2017) by Orticanoodles in Milan, Italy, revealing detailed information about its pigments, binders, fillers, and degradation. The findings demonstrate the potential of this integrated methodology for the effective material identification, conservation assessment, and short-and long-term monitoring of urban heritage.

street art | paint materials | non-invasive in-situ spectroscopic methods | hyperspectral imaging | UAS multispectral imaging

Significance

This paper presents a pioneering multimodal, multitechnique, and multiscale analytical methodology for studying the materials in street art murals. By combining in situ noninvasive analyses with laboratory analytical techniques applied to microsamples, this work offers a comprehensive approach to investigating the composition of paints in street art. The study introduces an innovative multianalytical procedure from in situ high-specific point chemical analysis to advanced imaging techniques like hyperspectral imaging and multispectral imaging via drone. This combination of techniques offers insights into the chemical makeup of street art over large surfaces up to tens of square meters. The ability to assess and monitor the materials in street art more comprehensively opens the door for future studies on the degradation mechanisms of murals.

Street art has emerged as an artistic expression, overcoming the physical confines of art galleries and museums. The roots of mural creations can be traced back to prehistoric times, when humans adorned the walls of the caves with graffiti. The 1960s marked the emergence of contemporary outdoor murals, with the first examples appearing in the suburban areas of the main metropolitan cities in the United States (1). It is only in the last years that the perception of urban art has radically changed, recognizing its power to transform neglected urban landscape spaces into requalified cultural heritage sites. Street murals have also become a medium for political or social commentary, a way to memorialize historical events. The artist's concept of street art is that it is inherently transient; it exists temporarily, subject to being painted over at any time. The exposure conditions in which they are created emphasize their ephemeral character (2). Nevertheless, the social awareness toward urban contemporary art and the need to preserve it in its context are widely recognized today (3).

The conservation of street art murals is highly challenging, considering the heterogeneity and fugitivity of the painting materials, the environmental factors to which they are constantly subjected, and possible acts of vandalism (4). Moreover, the monumental scale of most murals, often placed in difficult-to-access locations, necessitates highly specialized and costly instrumentation and expertise, adding to the complexity of conservation interventions.

Thus, the first necessary step to outline effective monitoring strategies and plan suitable conservation and protection treatments is characterizing the paint materials and investigating their stability in outdoor environments. A wide plethora of paint formulations are nowadays available and employed in murals, and many studies reported

This article is a PNAS Direct Submission. A.M. is a guest editor invited by the Editorial Board.

[1]Present address: Department of Earth and Environmental Sciences, University of Milano-Bicocca, Milan 20126, Italy.

[2]Present address: Inter University Consortium, Casalecchio di Reno, Bologna 40030, Italy.

[3]Present address: Department for Humanistic, Scientific and Social Innovation, University of Basilicata, Potenza 85100, Italy.

[4]Present address: Department of Chemical Sciences, University of Naples Federico II, Napoli 80126, Italy.

[5]To whom correspondence may be addressed. Email: laura.cartechini@cnr.it.

This article contains supporting information online at https://www.pnas.org/lookup/suppl/doi:10.1073/pnas.2504918122/-/DCSupplemental.

Published August 25, 2025.

in the literature are devoted to their characterization in terms of composition (5–10), and chemical and physical stability (11–17) in reference materials or mock-ups. While some studies have been reported on the characterization of the paint constitution of samples taken from street art murals (18–24), only a small number of in situ investigations have been carried out and were limited by the use of a few analytical techniques (7, 25–27). At present, the need to bring noninvasive spectroscopic point techniques to multispectral and hyperspectral imaging to obtain molecular information from large painted surfaces, like mural paintings, has become increasingly recognized in field studies (28, 29). To address this, stand-off imaging methods for remote sensing of murals in challenging or inaccessible locations have been proposed. These methods include the use of compact, lightweight hyperspectral cameras (30, 31) or spectral imagers paired with telescopes (32). On the other hand, drone-based remote sensing is emerging as a promising tool for heritage science, mostly for surveying archaeological sites. Compared to traditional satellite or aircraft platforms, drones offer a more cost-effective and time-efficient solution, minimizing the impact of research budgets and timelines (33). Drones can be equipped with multispectral, hyperspectral imagers and thermal sensors for terrestrial archaeological investigations (34). However, there is significant potential to expand their use in developing innovative approaches for the study and preservation of various types of cultural heritage artifacts.

In this study, the first in situ campaign on a street art mural was conducted by employing a wide range of spectroscopic techniques spanning from X-rays to the visible, near-short wave, and medium infrared (VIS-NIR-SWIR-MIR) regions. This approach combined information from highly specific point chemical analysis, which was scaled up to selected areas through hyperspectral imaging using an aerial work platform and further extended to the entire painted surface through multispectral imaging analysis via a drone (unmanned aircraft system-UAS).

Targeted sampling for further chromatographic and spectroscopic analysis is reported. Specific research was carried out on the postprocessing of the hyperspectral and multispectral datasets, optimizing the equalization procedure of the data cubes before their stitching to achieve consistent analysis and comparison of the results.

The investigated mural painting "Musica Popolare" belongs to a collection of urban artworks entitled "OrMe"-Ortica Memoria by artistic collective Orticanoodles (Milan, 2017). The artwork was selected within the project PRIN-2020 SUPERSTAR-*Sustainable Preservation Strategies for Street Art*-(https://prin2020superstar.dcci.unipi.it) in collaboration with local public institutions and the Museum of Cultures of Milan (MUDEC). Musica Popolare is a very peculiar and iconic mural that belongs to the urban pictorial art project involving the entire Ortica neighborhood. The artwork embodies the collective historical memory and identity of one of Milan's oldest and most vibrant neighborhoods. Its realization aims to requalify the urban space, transforming it into an open-air museum through the collaborative efforts of both citizens and public institutions. The mural's cultural and social significance underscores the importance of transmitting it to future generations, highlighting the need for planned initiatives aimed at its preventive conservation. The mural suffers physical and chromatic alterations (mainly fading) due to exposure to the outdoor environment and its location at a railway overpass (4). The information collected with the multimodal approach provided a comprehensive view of the materials and their state of conservation across an extended surface.

Results

The Case Study. The selected case study is the mural Musica Popolare made by Orticanoodles in 2017 in the suburbs of Milan in collaboration with the cultural association OrMe-Ortica Memoria (https://www.mudec.it/2022/05/11/orme/ and https://orticamemoria.com/). The work is a tribute to the most prestigious and loved artists of the Milanese culture and song: Ornella Vanoni, Enzo Jannacci, Dario Fo, Ivan Della Mea, Giorgio Strehler, Giorgio Gaber, and Nanni Svampa (Fig. 1*A*). The mural is located at a railway overpass and was executed both on the walls of the tunnel and outside it. The different exposure of the painted surface to environmental and anthropic agents (e.g., sunlight, rain, pollutants, and temperature change) has determined significant alteration of original colors, visible mainly in the faded red tones in the outside surface (Fig. 1 *B* and *C*) (4).

The in situ study was carried out in September 2022 and consisted of noninvasive spectroscopic point analyses of both the exposed and not exposed mural surfaces complemented by targeted laboratory analyses of nine microsamples collected from the detached pictorial film corresponding to different colors (sample name, description, and location are reported in *SI Appendix*, Table S1). Multispectral and hyperspectral imaging allowed the analytical information to be extended to the entire mural painting, although only the exposed surface was analyzed due to the limited space under the overpass that prevented the use of stand-off imaging techniques.

Material Identification. The analytical information achieved from the combined use of noninvasive elemental and molecular spectroscopies (more than 70 point measurements using external reflection Fourier transform infrared spectroscopy (FT-IR), Raman spectroscopy, VIS-NIR-SWIR reflectance spectroscopy, and X-ray fluorescence spectroscopy-XRF), integrated with the analysis of the microsamples by micro-Raman spectroscopy, pyrolysis gas chromatography–mass spectrometry (Py-GC–MS) and liquid chromatography coupled with diode array detector (HPLC–DAD) and tandem mass spectrometry (HPLC–MS/MS), allowed for a comprehensive characterization of the painting materials. Table 1 summarizes the identified pigments and fillers. Raman spectroscopy analyses, carried out in situ and on the microsamples, were pivotal for pigment identification with the support of VIS-NIR-SWIR and XRF spectroscopies. Organic synthetic pigments, recognized as Pigment Red 112 (PR112 C.I.12370) and Pigment Yellow 83 (PY83, C.I.21108), were used by the artists to modulate the different hues of the red, yellow, and brown colors. These pigments were mixed with titanium dioxide (found ubiquitous by XRF and identified mainly in the rutile form by Raman) or iron oxides (mainly as pigments equivalent to the mineral forms of hematite and goethite) to modify light and dark tones, for a total of thirteen identified paints (red, pink, dark red, dark brown, brown, light brown, beige, light yellow, dark yellow, orange, white, light gray, and gray). Phthalocyanine Pigment Blue (PB15, C.I.74160) was also identified in the very dark brown. Fig. 2 *A* and *B* shows the Raman spectra collected on the microsamples *Red-01* and *Dark-Brown-05* and the corresponding spectra from the in situ analysis compared with reference spectra acquired at the same laser wavelength on standards of the identified pigments. The comparison evidenced the copresence of PR112 and PY83 in the sample *Red-01* (Fig. 2*A*) and of hematite and PB15 in the sample *Dark-Brown-05* (Fig. 2*B*) (35). Furthermore, HPLC–DAD and HPLC–MS/MS identified Pigment Violet 19 (PV19, C.I.73900) in the microsample *Red-01,* which, indeed, comes from a red area with a pinkish hue.

Fig. 1. Photographs of the mural Musica popolare (https://www.mudec.it/2022/05/11/orme/) made by Orticanoodles in 2017. (*A*) position of the investigated areas within the entire mural surface (*B*) under the railway overpass (*Nanni Svampa*), and (*C*) outside it (*Enzo Jannacci* and *Dario Fo*).

FT-IR spectroscopy detected kaolin, calcite, quartz, and talc as fillers/extenders of the paints. In addition, this technique enabled the noninvasive identification of the main organic components of the paints (Fig. 3), evidencing in all the spectra the diagnostic bands of a styrene resin ($\nu(CH)_{Ar}$ above 3,000 cm^{-1} and the in-plane ring breathing modes (C=C stretching) at about 1,600 cm^{-1}) (36) and the presence of a vinyl component prevalently in the red points ($\delta(CH_2/CH_3)$ at about 1,375 cm^{-1} and ν(C–O–C) at about 1,250 cm^{-1}) (37). Interestingly, from the inspection of the short-wave infrared region (SWIR), more sensitive to subsurface/bulk paint components (37, 38), the profile shape of the $\delta+\nu$(C-H) combination bands in the range 4,400 to 4,200 cm^{-1} suggests the presence of an alkyd resin (37). The alkyd component, not detected in the mid-IR range, can be attributed to a preparation/paint layer underneath the surface styrene/vinyl-based paint layer.

A distinct marker of surface degradation was the detection of oxalates by FT-IR (39), which are present regardless of surface exposure. These compounds are widespread products of painting surface decay in outdoor and indoor conditions for different types of substrates; nevertheless, their origin is still debatable, whether related to microbiological attack, environmental contaminants, or oxidative degradation of organic components (40). In this specific study, the observation of oxalates distributed over the entire mural surface does not denote a specific effect of environmental exposure on their formation.

Although the red and yellow colors outside the underpass appeared less vivid than those inside, no significant spectral differences were observed by Raman and FT-IR spectroscopy as indicators of a distinct decay. More specifically, FT-IR evidenced a decrease in the contribution of quartz and an increase of a shoulder around 1,205 cm^{-1} (marked with an asterisk in Fig. 3). This band relates very well with the ν(C-O-C) stretching of an acrylic component as detected on the samples by Py-GC–MS (see *Discussion* below and Table 2). It is possible that the thinning/degradation of the exposed paint surface helped the spectral contribution of this binder component to increase.

FT-IR and Raman results were validated and integrated by Py-GC–MS, HPLC–DAD, and HPLC–MS/MS analysis, which permitted the unambiguous identification of paint binders, organic additives, and pigments in 8 analyzed microsamples (location and description in the *SI Appendix*, Table S1), as summarized in Table 2.

The Py-GC–MS profiles obtained for the sample *Red-01* (Fig. 4*A*), *Light-yellow-08* (Fig. 4*C*), and *Dark-yellow-09* highlight the presence of a styrene-acrylic resin as paint binder featuring methyl methacrylate (MMA), n-butyl acrylate (nBA), n-butyl methacrylate (nBMA) styrene monomers, and oligomers of styrene and styrene-MMA, as significant GC–MS peaks.

In addition, *Red-01* (Fig. 4*A*) presents a pyrolysis product of polyvinyl acetate (acetic acid) and two pyrolysis products of the red azo dye PR112 (1,2,4-trichloro-benzene and 2,4,5-trichloro-benzenamine) (8).

The binder detected in the samples *Dark-red-04* (Fig. 4*B*), *Dark-brown-05*, *Brown-06,* and *Light-brown-07* is still a styrene-acrylic resin but with a different formulation featuring in the pyrogram characteristic peaks associated with MMA, styrene monomers, and oligomers. Methenamine, a preservative additive, was also identified (41).

To rationalize the fading process affecting the red areas of the mural, two samples were collected from two different parts of the red paint surface (location and description in the *SI Appendix*, Table S1) for the mass spectrometric analysis of organic pigments: one from a faded area near the portrait of *Dario Fo*, which was directly exposed to sunlight and weather (*Red-01*), and the other from the inside of the railway overpass tunnel, in the section representing *Nanni Svampa* (*Red-03*). The analyses carried out by HPLC–DAD and HPLC–MS/MS allowed us to assess the presence

Table 1. Summary of the spectroscopic results from the in situ measurements on the mural and analysis of the samples by micro-Raman (sample name in brackets; see *SI Appendix* for sample descriptions)

Color	Paint color*	SAM color legend†	Noninvasive analysis	micro-Raman on samples
Red			PR112, PY83	
Pink			PR112, PY83	PR112, PY83 (*Red-01*) PR112 (*Red-02*)
Dark red			Iron-based pigment, PR112, PY83	Hematite (*Dark-red-04*)
Dark brown			Iron-based pigment, PY83, possible PB15	Hematite, PB15 (*Dark-brown-05*)
Brown			Iron-based pigment, PR112, PY83	Hematite (*Brown-06*)
Light brown			Iron-based pigment, rutile	Hematite, rutile (*Light-brown-07*)
Beige			Iron-based pigment, rutile	
Light yellow			Iron-based pigment, rutile	PY83, rutile (*Light-yellow-08*)
Dark yellow			Iron-based pigment	Goethite, rutile (*Dark-yellow-09*)
Orange			PR112, PY83, iron-based pigment	
White			Rutile, calcite	
Light gray			Ti	
Gray			Ti, Cu, carbon black	
Filler/Extender			Kaolin, talc, quartz, calcite (also as substrate)	

*The color images of the paints are from optical photographs.
†The color legend is the same as the plots of the results from the Spectral Angle Mapper (SAM) analysis.

of two synthetic organic pigments, PR112, already identified by Py-GC–MS, and PV19 in both samples. PR112 was also detected in situ and in the samples *Red-01* and *Red-02* by Raman analysis.

It is interesting to compare the molecular profile in terms of the organic pigments detected in the sample collected from the area of the mural shadowed by the tunnel, with those from the area exposed to direct sunlight and weathering agents. In the HPLC–MS/MS chromatogram of *Red-03*, collected from the area of the mural that was covered by the tunnel and thus protected from environmental factors (e.g., sunlight and rain), two peaks associated with the molecular ions of PR112 (*m/z* = 482.016) and PV19 (*m/z* = 311.083), respectively, were detected (Fig. 5*A*). Conversely, in *Red-01*, collected from the exposed and faded surface, along with the same two main pigments, also two possible oxidation products of PR112 were detected, as hypothesized on the basis of their molecular formula, exact mass value, and isotopic cluster typical of a three-chlorides-containing compounds ($C_{17}H_{10}Cl_3N_3O_2$, *m/z* = 392.970 and $C_{17}H_9Cl_3N_2O_3$, *m/z* = 393.995) (Fig. 5*B*). These latter species are likely degradation products of PR112, formed through photo-oxidation in areas exposed to light. Thus, their formation may have been limited to the micrometric upper layer of the paint surface. Given that HPLC–MS/MS is a bulk analytical technique, these degradation compounds are expected to be present at lower concentrations compared to the original PR112, which remains in relatively higher amounts. Nevertheless, the detection of these degradation products offers a plausible explanation for the observed fading phenomena.

Hyperspectral Imaging and Multispectral Imaging on UAS: Implementation of the Upscaling Methodology and Results. Molecular information provided by HSI was used to discriminate and map the different paints on the basis of their composition, as determined through integrated in situ and laboratory analyses. Data processing for calibration, equalization, and stitching of the hypercube datasets is described in the *Materials and Methods* section. The mural's overall composition was, then, reconstructed by SAM analysis applied to the complete stitched hypercube. The spectral interval was restricted to 385 to 700 nm with respect to the operational range of the camera to avoid spectral artifact due to the use of natural environmental light as a source (as described in

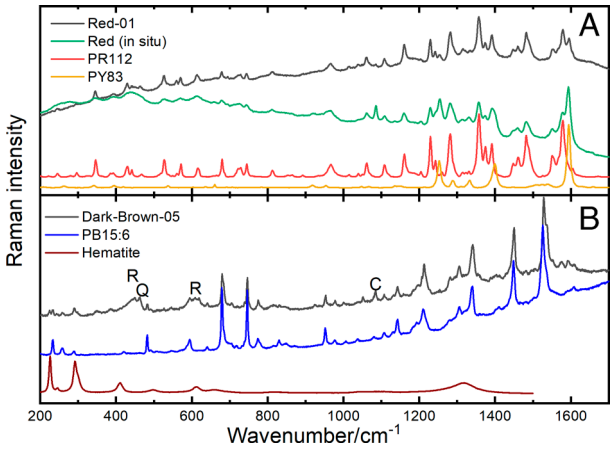

Fig. 2. Raman results. Raman spectra (785 nm) collected on samples (*A*) *Red-01*, compared with the in situ measurement on the exposed red area, and (*B*) *Dark-Brown-05*. Reference Raman spectra (785 nm) of PR112, PY83, PB15:6 (35), and hematite are also reported. R: rutile, C: calcite, Q: quartz. Spectra are offset along the *y*-axis for clarity.

the Experimental Methods section) (42). The spectra from the HSI dataset that were considered relevant as endmembers for spectral classification of each of the identified thirteen paints are detailed in *SI Appendix*, Fig. S1. The selected endmembers for the SAM analysis were validated by comparison with reflectance spectra collected by point analysis in the 350 to 2,500 nm range for the different paints (shown in *SI Appendix*, Fig. S2). Orange and yellow paints were all characterized by VIS-NIR reflectance signals ascribable to yellow iron hydroxide (compatible with the mineral pigment goethite). The spectra recorded on the orange tonalities showed additional signals indicative of the presence of naphthol red PR112. The same red pigment was detected in red, pink, and dark red areas with spectral profiles showing distinctive absorption minima around 515 to 525 nm and 545 to 554 nm, matching a reference sample of the synthetic pigment. Iron oxide-based pigments were added to obtain darker tonality. Indeed, spectra collected on dark red areas show reflection maxima and absorption minima compatible with the mineral pigment hematite. Iron-based pigments (oxides and hydroxides) have been suggested to be present also in brown tonalities (43).

Fig. 6 plots show the average spectra and SD of the endmembers selected to classify each paint of the mural by SAM analysis

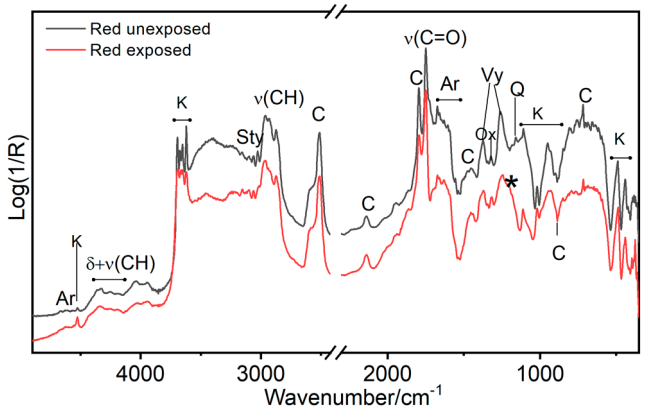

Fig. 3. FT-IR results. External reflection FT-IR spectra collected on red areas inside and outside the underpass with the assignment of the vibrational bands of the identified paint components. Ar: aromatic component (from the binder and the organic pigments); K: kaolin; Sty: styrene component from the binder; C: calcite; Ox: oxalates; Vy: vinylic component from the binder; Q: quartz. The asterisk marks a spectral contribution present on the exposed paint surface (see text).

Table 2. Paint binders, organic additives, and pigments identified by microdestructive techniques (Py-GC–MS, HPLC–DAD, and HPLC–MS/MS) in eight samples collected from the mural

Sample	Binders	Organic additives	Organic pigments
Red-01	Polyvinyl acetate and styrene- acrylic (acetic acid, MMA, nBA, nBMA, styrene, styrene oligomers, styrene-MMA oligomers)	n.d.	PV19, PR112 and its degradation products
Red-03*	–	–	PV19, PR112
Dark-red-04 **Dark-brown-05** **Brown-06** **Light-brown-07**	Styrene- acrylic (MMA, styrene, styrene oligomers)	Methenamine	n.d.
Light-yellow-08 **Dark-yellow-09**	Styrene-acrylic (MMA, nBA, nBMA, styrene, styrene oligomers, styrene-MMA oligomers)	n.d.	n.d.

*Analyzed only by HPLC–DAD and HPLC–MS/MS due to the tiny amount of sample.

of the HSI dataset. The range of variability of the spectra sampled as endmembers is expressed by their SD. Fig. 6 maps display the summed SAM distributions of each endmember. With this supervised approach, the precise chemical identification of the paint materials is converted by the SAM analysis into chemical maps where the paints used by the artists are identified and separated with satisfying accuracy.

Nevertheless, some areas in the maps of Fig. 6 are not classified or misclassified; this is the case of some very dark (such as dark brown and gray) or very light shades (such as white, light yellow, and light gray) that have less resolved spectral features. Furthermore, there are algorithm imperfections ascribable to the spectral heterogeneities related to the variable environmental light exposure conditions, which were not fully addressed by the spectral hypercube correction process and data treatment (see the Materials and Methods section). This is the case, for example, of the two data cubes in correspondence with the lower part of the nose of *Dario Fo* in Fig. 6.

In this phase of the research, a multispectral imaging camera was employed for the UAS survey and to scale up analytical information across the entire mural surface. The decision to use a multispectral sensor instead of a hyperspectral system allowed for a straightforward evaluation of both the data acquisition and upscaling methodology, albeit with some compromise in spectral data quality. However, this choice offered several advantages: the equipment was more readily available and cost-effective, data processing was simplified, and spectral data correction was more manageable in the presence of environmental lighting variability, particularly given the significantly higher number of spectral cubes collected from the air.

The use of a GPS system during the acquisitions allowed the reconstruction of a three-dimensional model of the artwork using the Structure from Motion (SfM) technique (44–47). The results

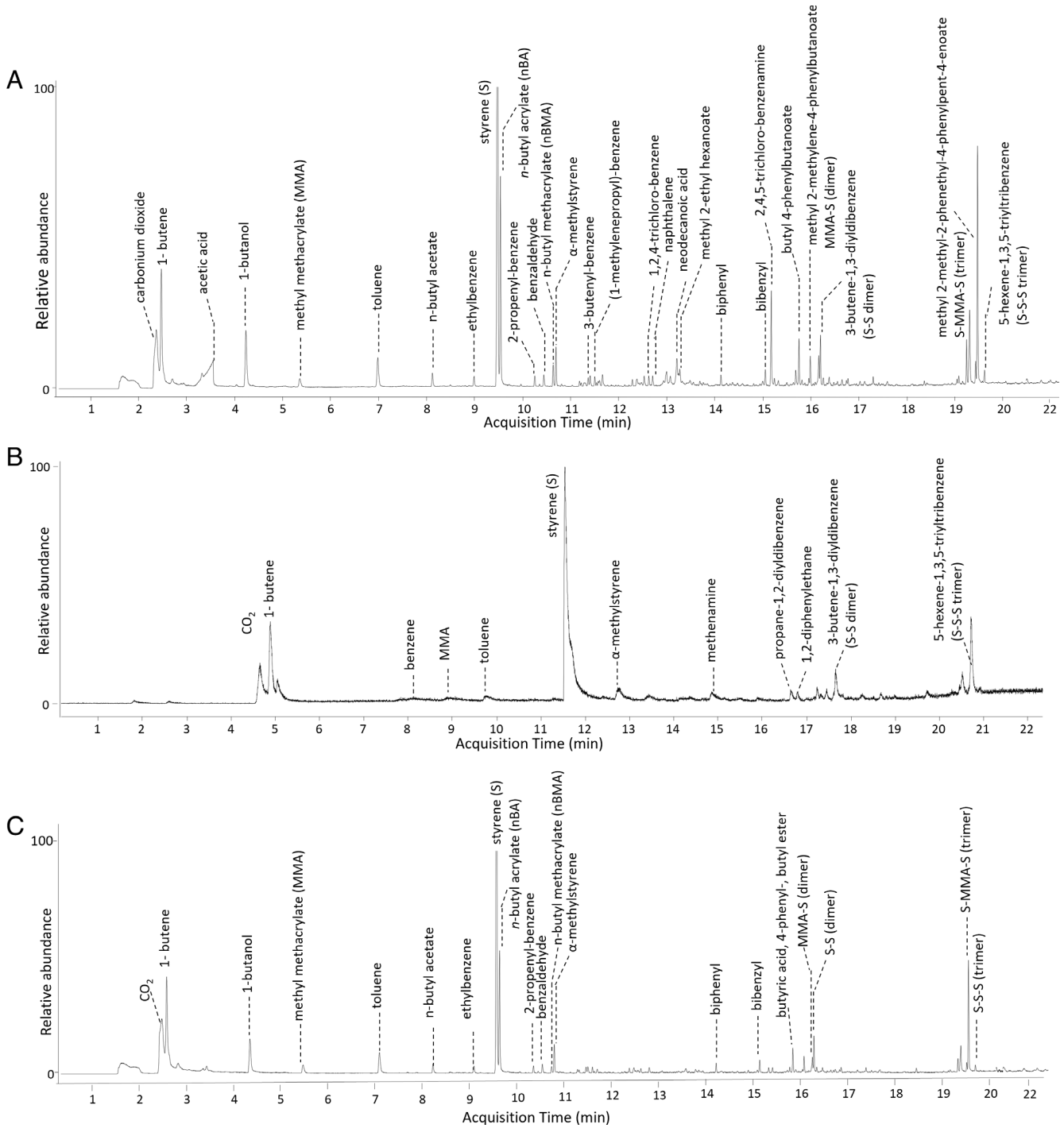

Fig. 4. Py-GC–MS results. Pyrograms of (*A*) Red-01; (*B*) Dark-red-04; and (*C*) Light-yellow-08.

of the SfM process applied to the multispectral images after radiometric correction and irradiance normalization were i) a georeferenced high-density point cloud, ii) a three-dimensional model (*SI Appendix*, Fig. S3*A*), and iii) an orthophoto mosaic (*SI Appendix*, Fig. S3*B*) of the mural painting. Following the processing of the HSI dataset, thirteen endmembers were identified. For each endmember, a 3x3 pixel window was used to sample the spectra within the acquired multispectral data at the same positioning as the HSI dataset. The extracted spectra and corresponding SD are shown in *SI Appendix*, Fig. S4. Spectral classification of the entire data cube was then performed by SAM using the selected endmembers; results are shown in Fig. 7 where the comparison with the SAM analysis of the HSI dataset is also shown. Despite the low spectral resolution of the multispectral dataset, the color classification is quite excellent and capable of reproducing the different hues of the principal paints in accordance with HSI results. Furthermore, the MSI dataset shows less sensitivity to environmental light conditions than the HSI dataset. This is likely due to the use of a sunlight incidence calibration sensor during each MSI acquisition. In contrast, in the case of the HSI data, only a few measurement repetitions of the gray standard were performed for calibration at the same light conditions as the analyzed surface due to operative constraints.

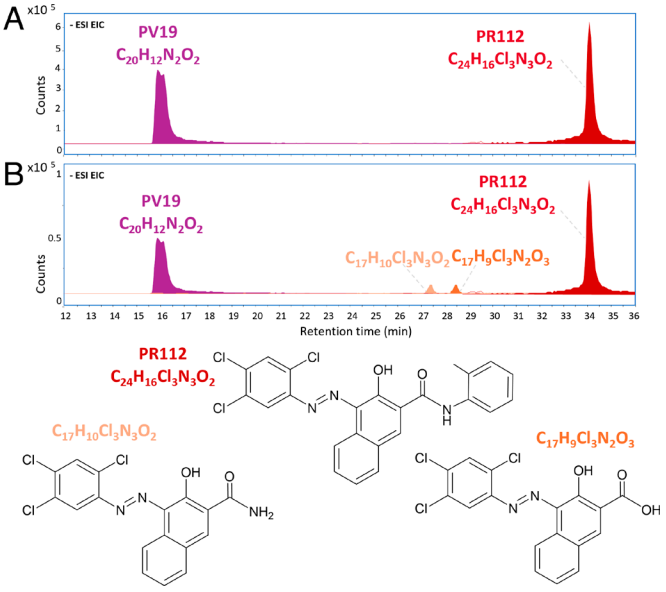

Fig. 5. HPLC–MS/MS results. Extract ion chromatograms (EIC) of PV19 ($C_{20}H_{12}N_2O_2$), PR112 ($C_{24}H_{16}Cl_3N_3O_2$), and its degradation products ($C_{17}H_{10}Cl_3N_3O_2$ and $C_{17}H_9Cl_3N_2O_3$) from the DMSO extract of the samples (*A*) *Red-03* and (*B*) *Red-01*. Negative acquisition mode. On the *Bottom*, the structure of PR112 and its hypothesized degradation products.

Discussion

The multiscale and multitechnique approach used to study the mural painting Musica popolare provided a body of analytical information that was rationalized and made usable by transferring the highly specific chemical information obtained locally to the entire painting surface through chemical maps. The process is based on the sequential treatment of the data blocks, where the material identification provided by point analyses and the study of microsamples drove the interpretation and processing of the HSI and MSI results.

As a first step, the in situ spectroscopic analyses supported by microsample characterization clarified the complex composition of the mural paints in terms of the inorganic/organic pigments and fillers, binders, and possible related degradation products (Tables 1 and 2). Styrene and vinyl were detected as the binders, and an indication of the presence of acrylic and alkyd components was also found. This latter seems confined to the deeper layers, as revealed by FT-IR spectroscopy in the SWIR range, where a greater penetration depth of the probed volume is achieved (37, 38). The identification of the paint binders was fine-tuned thanks to Py-GC–MS, disclosing the use of polyvinyl acetate and styrene-acrylic (MMA, nBA, nBMA, styrene, styrene oligomers, styrene-MMA oligomers) resin.

The chromatic palette corresponding to the thirteen identified paints comprises synthetic organic pigments, including PR112, PV19, PY83, and PB15, combined with the use of Fe oxide-based pigments (such as hematite and goethite) and TiO_2 (mainly in the form of rutile) as a white pigment. Kaolin, calcite, quartz, and talc were identified as fillers/extenders of the paints.

Spectral profiles of the HSI datasets revealed features associated with the chemical nature of the paint chromophores. This information enabled the reconstruction of the paint distributions according to the compositions determined by the integrated in situ and laboratory-based methods. The endmembers identified for the different paint compositions and used in the SAM analysis of

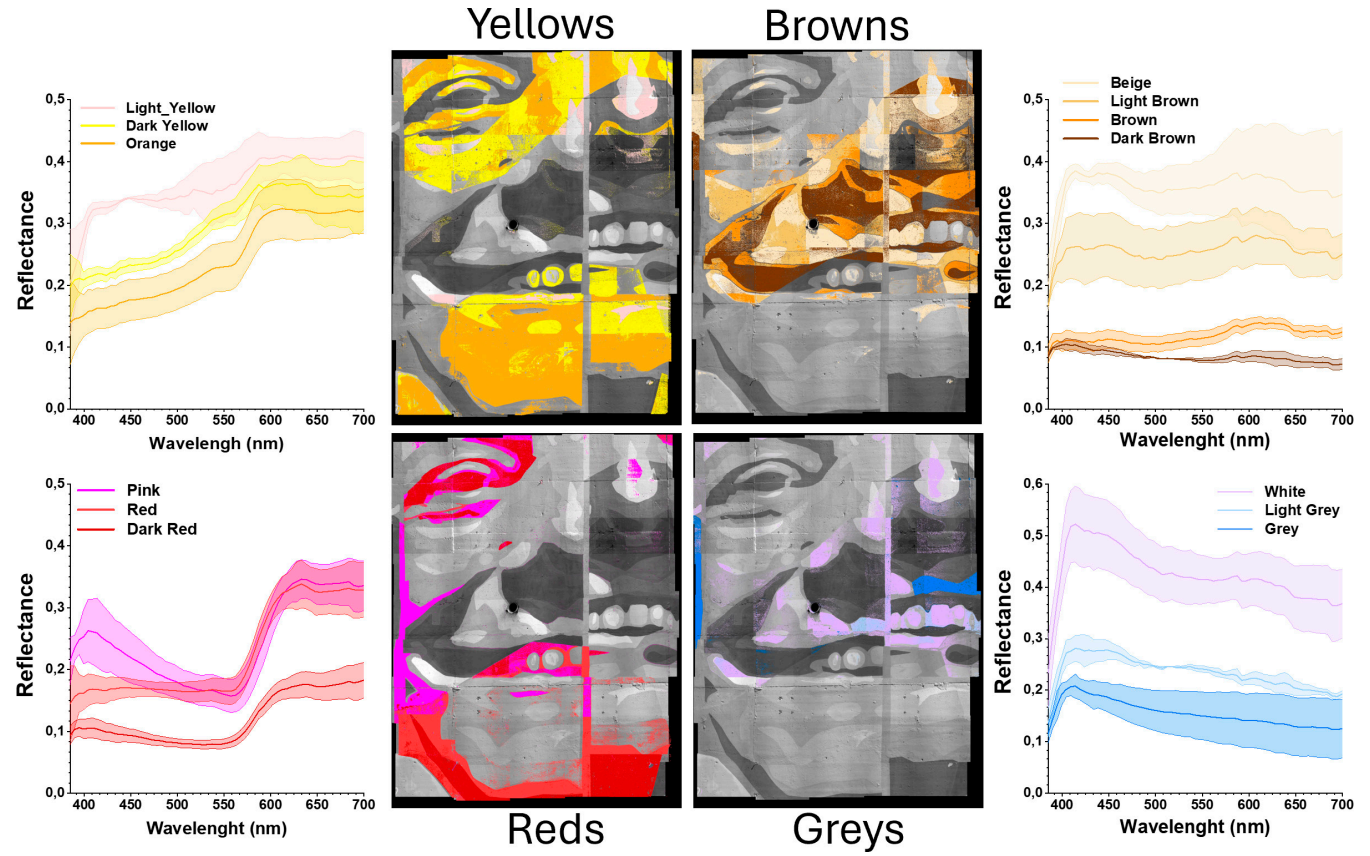

Fig. 6. SAM results for the principal color shades of the HSI dataset: yellows, browns, reds, and grays. Several endmembers were considered for each of the thirteen identified paints; the endmember plots show the mean spectra of each color and its SD.

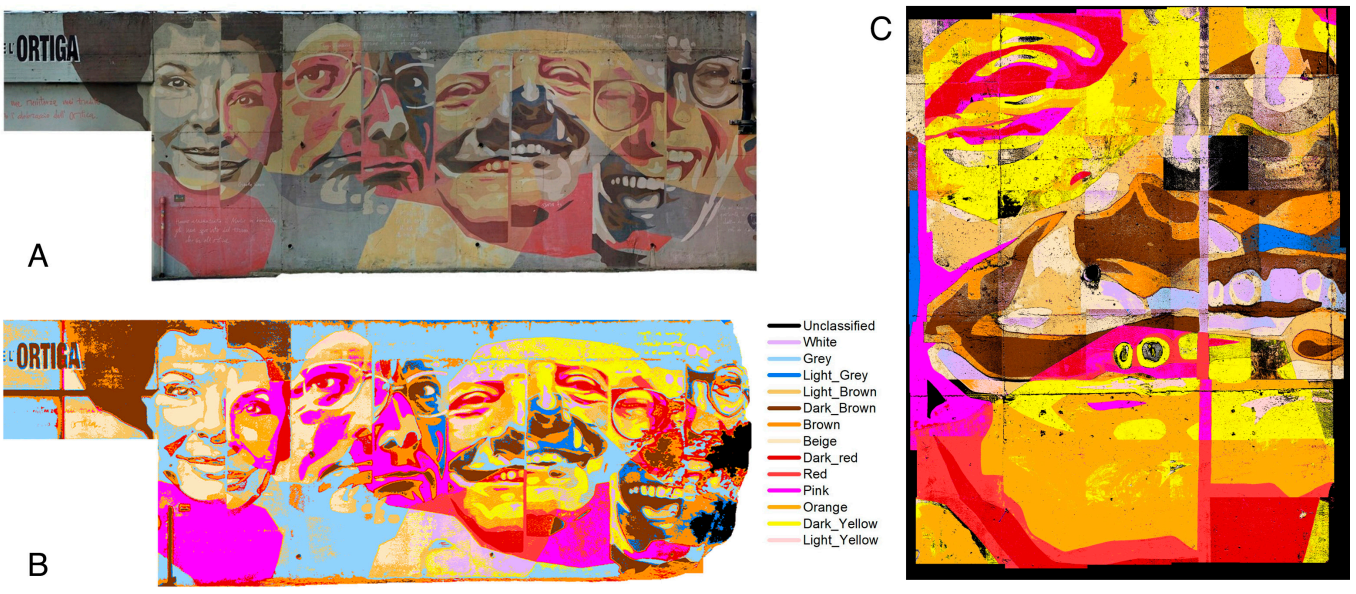

Fig. 7. Comparison of the SAM results. (*A*) Orthophoto mosaic and (*B*) corresponding SAM results for the MSI dataset compared with (*C*) the SAM results of the HSI dataset. Color legend and sampling positions of the endmembers are the same for the two datasets.

the HSI datasets enabled the classification of the whole investigated paint surface with good accuracy (Fig. 7*C*). Endmember selection played a critical role in obtaining comparable compositional maps from the SAM spectral classification of both HSI and MSI data cubes. This process allowed for the scaling-up of analytical information to cover the entire mural surface surveyed by the UAS, yielding satisfactory results, as shown in Fig. 7*B*. Interestingly, in the figure, the faded red areas are recognized and appear not uniform in correspondence to different degrees of fading, as in the pinkish-red background of Dario Fo (Fig. 7 *B* and *C*). To more effectively assess the cameras' sensitivity to color variations, conducting HSI and MSI analyses beneath the overpass would have been valuable. Unfortunately, due to the narrow space on the walking path and the impossibility to close the road to traffic, these analyses could not be carried out. However, a noticeable difference can be observed between the colors of the faded paint surface exposed to weathering agents (sunlight, rain, etc.) outside the overpass and the surface inside it (Fig. 1 *B* and *C*). This is visible mainly in the exposed faded pinkish-red areas containing the synthetic organic pigments PR112 and PV19 (Table 2). These pigments are stable to light aging in the UV and visible range as pure powder, while they may significantly impact the photostability of the synthetic binder toward oxidative degradation processes (48, 49). The higher light stability of the paint containing PV19 with respect to PR112 has been proven by colorimetric tests carried out on artificially aged styrene-acrylic copolymer mock-ups (50). In addition, the photoinstability of PR112 has recently been observed in red faded areas of the "20 y of Freedom and Democracy" mural (27). This possibly explains our HPLC–MS/MS results which highlight the presence of oxidation products of PR112 in the faded red areas of the outdoor mural exposed to sunlight. Additional factors may have contributed to the fading of the mural. The presence of titanium dioxide (rutile), identified through a combination of Raman and XRF spectroscopies, may have further promoted the photodegradation of the organic pigment. This white pigment/filler is known for its high sensitivity to both UVA and visible radiation, enhancing its role in light-induced deterioration processes (50–52). The photoreactivity of titanium dioxide may also have contributed to the so-called chalking effect of the binder's polymeric phase (53, 54). This phenomenon involves the photo-oxidation of the binder in the upper paint layer, accompanied by the degradation of synthetic organic pigments. These pigments typically have smaller particle sizes than their inorganic counterparts. As a result, unbound inorganic white pigments and fillers become predominant on the surface, leading to a noticeable loss of gloss (4, 27). This effect may be exacerbated by the embrittlement of the polymeric binder, which can cause the underlying preparatory layer to become visible. The understanding of the complex mechanisms underlying color fading in urban muralism undoubtedly warrants further investigation. However, in the specific case study examined here, our results, although not definitive, provide valuable insights into the observed fading phenomena and serve as a stimulus for continued research.

Conclusions

The paper proposes a multiscale multimodal analytical approach to achieve a comprehensive view of the paint materials and their state of conservation over an extended surface in the context of mural paintings in urban and street art. This work represents the first proof of concept study, tested on the iconic mural painting Musica Popolare in Milan, to explore the scalability of the analytical information obtained with localized analyses to extend it to a selected area (15 m^2) using hyperspectral imaging, and, subsequently, to the full mural surface (397 m^2), which was scanned using multispectral imaging via UAS. The decision to conduct the aerial survey using a multispectral camera was driven by the need to test a more affordable and user-friendly tool—accessible to a wider community—compared to a hyperspectral set-up, which features higher operational costs, more complex data processing, and limited accessibility for many stakeholders.

Localized spectroscopic analysis during the in situ campaign, integrated with mass spectrometric and micro-Raman analysis of a few microsamples, provided highly specific analytical information according to a diagnostic methodology well-established in the collaborating research groups. HSI data acquisitions were exploited to scale up the analytical information to cover a square-meter surface and classify painting materials by SAM analysis according to their spectral profiles in the visible range using

sunlight as the radiation source. The implementation of the same data processing by SAM analysis of the MSI dataset acquired by UAS provided a further enlargement of the probed surface with the classification of the paints of the mural Musica Popolare according to the identified materials.

The research involved considerable logistical efforts for the in situ collection of spectroscopic datasets, as well as extensive work for the elaboration of HSI and MSI data. Despite these challenges, the results from the HSI and MSI analyses are highly promising for the chemical survey of large painting surfaces. This suggests that, in the future, once an initial accurate diagnostic campaign is completed, MSI by UAS could be used to monitor the progression of paint alterations across substantial portions of the surface. With the advantage of low cost and ease of use, it would allow for identifying varying responses to exposure to specific environmental factors. From another perspective, the UAS survey serves as a powerful tool for the preliminary evaluation of materials and the conservation status of street art murals. It can help direct more targeted analyses to critical areas and, if necessary, guide the planning of microsampling for subsequent laboratory analysis.

The overall workflow is still being optimized, particularly regarding the acquisition of HSI data to produce better-equalized hypercube sets before analysis. Additionally, ongoing improvements to the instrumentation are focused on integrating a UAS equipped with a hyperspectral camera. This will allow for the transfer of HSI measurements from ground to aerial mode, enabling the coverage of larger surfaces in significantly less time. In this perspective, the experience gained from applying hyperspectral imaging with a conventional terrestrial camera was essential for identifying the challenges of working outdoors under variable lighting conditions and for establishing effective procedures to correct spectral data through supervised processing.

In a future vision, the study and monitoring of urban artworks could be managed through a circular process of analytical data acquisition—optimized for resource efficiency, analysis time, and staff training. This process would integrate well-established investigative techniques, commonly used in museum settings and conservation laboratories, with drone-acquired multispectral and/or hyperspectral data that represent the entire surface of the work. By linking point, specific, high-resolution analyses with comprehensive aerial surveys, this approach could offer a scalable and systematic model for urban art conservation. The proposed concept of a multimodal and multiscale approach ensures the versatility required to be effectively applied across diverse contexts and to address the specific challenges presented by the artworks under study.

Materials and Methods

X-ray Fluorescence Spectroscopy. X-ray fluorescence (XRF) measurements were carried out using the portable spectrometer ELIO (Bruker Optics, Germany/USA-MA). The instrument is equipped with an Rh X-ray tube and an SSD detector with energy resolution < 140 eV for Mn Kα. The X-ray beam is collimated onto the sample surface with a pinhole of 1 mm in diameter at a working distance of 1 cm. During measurements, the X-ray tube was operated at 40 kV and 100 μA, and the acquisition time was 40 s per spectrum.

External Reflection FT-IR Spectroscopy. For external reflection FT-IR measurements, a portable spectrometer (ALPHA, Bruker Optics, Germany/USA-MA) equipped with a SiC Globar infrared radiation source, a Michelson interferometer (RockSolid™ design), and a room-temperature DLaTGS detector was used. Pseudoabsorbance spectra [log(1/*R*), where *R* is reflectance] were obtained from areas of 6 mm in diameter by means of an external reflection module with specular optics (22°/22°), acquiring data in the range of 7400 to 345 cm^{-1} at a resolution of 4 cm^{-1} and for 145 scans. A flat gold mirror was used for the background correction.

VIS-NIR-SWIR Reflectance Spectroscopy. Reflection VIS-NIR-SWIR spectra were recorded using a portable spectroradiometer (FieldSpec4, Malvern Panalytical, UK). The instrument consists of three detectors: an array composed of 512 silicon elements covering the 350 to 1,000 nm spectral range and two InGaAs photodiodes for the 1,000 to 1,800 nm and 1,800 to 2,500 nm spectral range, respectively. The instrument spectral resolution is 3 nm in the VIS-NIR range (350 to 1,000 nm) and 10 nm in the SWIR range (1,000 to 2,500 nm). The instrument has a 1 m long optical fiber directly connected to the spectrophotometer with a 25° FOV. The measurements were carried out using external lighting consisting of a 12 V quartz-tungsten lamp with ventilated cooling placed at 45° with respect to the surface. The optical fiber collecting the signal, instead, was held perpendicular to the surface of the painting, at a variable distance depending on the investigated area. The working distance dictates the lateral resolution in this setup: The measurement area is indicatively half the working distance, and then the sampling area varies in diameter from 1 cm to 5 cm. For each sampling point, 50 spectra were averaged. A Spectralon™ white reference standard was used for white calibration.

Raman Spectroscopy. In situ Raman spectra were acquired by a portable spectrometer Xantus-2™ (Rigaku, Japan) equipped with two laser excitation lines (785 nm and 1064 nm) and a thermoelectrically cooled 2000 × 256 Pixel CCD detector. Measurements were carried out using a 785 nm laser, with acquisition times of 5 to 20 s, 3 to 5 accumulations, and power from a minimum of 30 mW to a maximum of 100 mW. The spectral resolution is 7 to 10 cm^{-1}, and the spectral range is from 200 to 2200 cm^{-1}.

For the analysis of microsamples, a confocal bench-top micro-Raman instrument (InVia™, Renishaw, UK) was used, equipped with a Leica microscope with 50× objective, 1200/1800 lines/mm diffraction grating and CCD detector. Measurements were conducted using an NdYAG laser (λ = 532 nm), a HeNe laser (λ = 633 nm), and a diode laser (λ = 785 nm). The laser power (1 to 3 mW) was appropriately chosen for each measurement to avoid sample degradation.

Analytical Py-GC–MS. Py-GC–MS analysis was carried out by a multishot EGA/PY-3030D pyrolizer (Frontier Laboratories Ltd., Fukushima, Japan) coupled with an 8890 gas chromatograph (Agilent Technologies, Palo Alto, USA) and with a 5977B mass selective single quadrupole mass spectrometer detector (Agilent Technologies, Palo Alto, USA). The pyrolizer interface was kept at 280 °C, the transfer line at 300 °C, and the valve oven at 290 °C. For the gas chromatographic separation, an HP-5MS fused silica capillary column (stationary phase 5% diphenyl–95% dimethyl-polysiloxane, 30 m × 0.25 mm i.d.), with a deactivated silica precolumn (2 m × 0.32 mm i.d.), both J Hewlett Packard (USA), was used. The split–splitless injector was used in split mode at 300 °C, with a split ratio of 1:20. The chromatographic conditions were as follows: 40 °C isothermal for 6 min, 20 °C/min up to 310 °C, and isothermal for 40 min. The carrier gas (He, purity 99.9995%) was used in constant flow mode at 1.0 mL/min. The observed m/z range of the mass spectrometer was 35 to 420. Mass spectra were analyzed with NIST MS Search 2.4 and/or compared with the available literature data and an in-house database of mass spectra. Before the analysis, the sample (ca. 90 μg) was placed in an inert stainless-steel cup and then flash pyrolyzed at 600 °C.

HPLC–DAD and HPLC–MS/MS. For HPLC–DAD analysis, a PU-2089 Quaternary Pump with degasser, equipped with an autosampler AS-950 and coupled to a spectrophotometric diode array detector MD-2010 (all Jasco International Co, Japan) was used. The working conditions were spectra acquisition in the 200 to 650 nm range every 0.2 sec with a resolution of 4 nm.

For HPLC–MS/MS analysis, an HPLC 1200 Infinity, coupled with a Quadrupole-Time of Flight tandem mass spectrometer 6530 Infinity by a Jet Stream ESI interface (Agilent Technologies, Palo Alto, USA) was used. ESI conditions: drying gas (N_2; purity>98%), temperature 350 °C, flow 10 L/min; capillary voltage 4.5 KV; nebulizer gas pressure 35 psig; sheath gas (N_2; purity>98%) temperature 375 °C, flow 11 L/min. High-resolution MS and MS/MS acquisition range was set from 100 to 1000 m/z in negative and positive mode with an MS and MS/MS scan rate of 1.04 spectra sec^{-1}; nozzle, fragmentor, skimmer, and octapole RF voltages were set at 1000 V, 175 V, 65 V, and 750 V, respectively. For the MS/MS experiments, 30 V was applied in the collision cell to obtain CID fragmentation (collision gas

N_2, purity > 98%). Agilent tuning mix HP0321 was used to calibrate the mass axis daily.

For both set-ups, the chromatographic separation was performed at 30 °C using a Poroshell 120 EC-C18 column (3.0 × 75 mm, 2.7 μm particle size) with a Zorbax Eclipse plus C-18 guard column (4.6 × 12.5 mm, 5 μm particle size), both Agilent Technologies (Palo Alto, USA). The gradient employed formic acid (FA) 0.1% v/v in LC–MS grade water (H_2O, eluent A) and FA 0.1% v/v in LC–MS grade acetonitrile (CH_3CN, eluent B). The flow rate was 0.4 mL/min, and the program was 15% B for 2.6 min, then to 50% B in 13.0 min, to 70% B in 5.2 min, to 100% B in 6.2 min, and then hold for 12 min; re-equilibration took 10 min. The injection volume was 20 μL and 5 μL for the HPLC–DAD and HPLC–MS/MS analyses, respectively.

The sample treatment consisted of the following steps: addition of 150 mL of DMSO, extraction in an ultrasonic bath at 60 °C for 1 h, filtration with PTFE syringe filters (0.45 μm pore size).

VIS-NIR Hyperspectral Imaging. The hyperspectral camera (SOC710, Surface Optics Corporation, San Diego, USA) utilizes a whiskbroom line scanner with 696 × 520 pixels. The acquisition covers the 385 to 1000 nm range with 128 spectral bands, reaching a spectral resolution of 4.5 nm. The camera mounts an objective with a focal length continuously adjustable by varying the lateral resolution.

The data portion of the artwork representing *Dario Fo* was acquired using a snake scan procedure and an electric scaffold positioned at about 4 m, achieving a lateral resolution of about 1 mm^2 pixel size for this acquisition. At these unusual acquisition conditions, the sun was used as an illuminant instead of an artificial light source. A total of 45 VIS-NIR hyperspectral cubes with dimensions of about 720 × 540 mm^2 were acquired with mutual overlap and arranged on five adjacent columns for a total height of approximately 5 m and width of 3 m, corresponding to about 15 m^2 in 90 min of net acquisitions (3 h considering the instrument arrangement on the platform).

As for the standard methodology, all the hypercubes were calibrated using a unique gray level standard. To standardize the illumination and reduce differences between the calibrated images, the cubes have been readjusted, adding or multiplying a constant factor to all the acquired wavelengths. This adjustment results in a more uniform brightness and contrast of the cubes. Data elaboration was carried out using custom Python-based scripts. Subsequently, the adjusted hypercubes were stitched using ENVI (Exelis Visual Information Solutions, Boulder, Colorado) without changing the brightness or contrast. Even if a consistent and homogeneous RGB result has been achieved after calibration, accurate spectral analysis of the total hypercube required additional steps. First, using the sun as a light source introduced peaks in the spectra response over the 800 to 1000 nm range that could not be entirely rectified. For this reason, the data analysis was performed limiting the spectral range to the 385 to 700 nm interval. Second, the total hypercube still presented some inhomogeneities due to spectral artifacts between areas painted with the same materials but belonging to different cubes. This may be due to the variable weather during the acquisitions, such as full sun or cloudy, which resulted in different illumination conditions. To address these deviations, the SAM analysis was performed by manually selecting more spectra considered relevant as endmembers for spectral classification of each of the identified thirteen paints (detailed in *SI Appendix*, Fig. S1). As the final step of the SAM analysis, all the imaging maps related to the same paint were summed. The ENVI software was used for the classification of the reconstructed hypercubes using the SAM algorithm.

Multispectral Imaging on UAS. A multispectral camera (Sequoia, Parrot, France) was adapted with a custom 3D printed mount on a drone (Phantom 4 RTK, DJI, China) and used for the acquisition. The multispectral camera is equipped with a photo sensor that acquires separate bands in the green (530 to 570 nm), red (640 to 680 nm), red edge (730 to 740 nm), and near infrared (770 to 810 nm) with 1280 × 960 pixel resolution and a visible camera with 4608 × 3456 pixel resolution. The system also has a sunlight incidence calibration sensor and a GPS.

For the mural Musica popolare, more than 1700 images were acquired at high mutual overlap (> 80%) at a constant distance from the artwork of about 5 m so that the three-dimensional model of the wall could be reconstructed and the textures well rendered. The drone acquisition took about 25 min and covered a surface area of about 60 m in length by about 8 m in height, totaling 397 m^2 of painted surface (excluding the tunnel opening).

Virtual artwork reconstruction operations were performed within the Agisoft Metashape software (v. 2.1.2), which allows i) application of radiometric correction and irradiance normalization to the images, ii) setting up of ground control points (GCPs) beaten with a high-precision GNSS to increase the accuracy and metric precision of the data, and iii) reconstructing a three-dimensional model of the artworks using the Structure from Motion (SfM) technique (44–47). The SfM process applied to the multispectral images resulted in a multiband (green to near infrared) orthophoto of the wall paintings, maintaining the spectral resolution of the input data and lateral spatial resolution. The data produced were then processed in the ENVI software for classification and identification of scene elements using the SAM algorithm and setting the classification to the same endmembers used for the hyperspectral dataset so that the data obtained could be correlated.

Data, Materials, and Software Availability. The authors declare that the data supporting the findings of this study are available within the paper and its *SI Appendix*. Raw data files are available in Zenodo (55).

ACKNOWLEDGMENTS. We are grateful to Marina Pugliese and Alice Cosmai of the Municipality of Milan–Direzione Cultura Area Museo delle Culture Progetti Interculturali e Arte nello Spazio Pubblico–for the support of the research. The researchers of National Research Council also acknowledge SHINE (Strengthening of the national hub of E-RIHS–European Research Infrastructure for Heritage Science) PON Ricerca e Innovazione 2014–2020 (CCI: 2014IT16M2OP005), the project H2IOSC (Humanities and cultural Heritage Italian Open Science Cloud), National Recovery and Resilience Plan (NRRP) Mission 4 Component 2 Investment 3.1 (Project code IR0000029) funded by the European Union–NextGenerationEU under the Italian Ministry of University and Research (MUR), and the Project PE 0000020 CHANGES (Cultural Heritage Active Innovation for Next-Gen Sustainable Society-CUP: B53C22003890006), NRRP Mission 4 Component 2 Investment 1.3, funded by the European Union-NextGenerationEU under the Italian MUR, for having supported part of the research activities. We also wish to express their gratitude to the Centre for Instrument Sharing of the University of Pisa for providing access to the pyrolysis – gas chromatography – mass spectrometry technique. This research was financed by the Italian PRIN2020 project SuPerStAr-Sustainable Preservation Strategies for Street Art, funded by the Italian MUR-Prot. 2020MNZ579.

Author affiliations: [a]National Research Council, Institute of Chemical Science and Technologies "G. Natta", Perugia 01623, Italy; [b]Centre of Excellence Scientific Methodologies applied to Archaeology and Art and Department of Chemistry, Biology and Biotechnology, University of Perugia, Perugia 06123, Italy; [c]National Research Council, Institute of Heritage Science, Area della Ricerca di Firenze, Sesto Fiorentino (FI) 50019, Italy; [d]National Research Council, Institute of Heritage Science, Tito Scalo (PZ) 85050, italy; [e]Department of Chemistry and Industrial Chemistry, University of Pisa, Pisa 56124, Italy; and [f]National Research Council, Applied and Laser Spectroscopy Laboratory, Institute of Chemistry of Organometallic Compounds, Research Area of the National Research Council, Pisa 56124, Italy

Author contributions: N.M. and L.C. designed research; F.S., B.D., A.R., M.S., I.D., B.C., and L.C. performed research; F.A., B.D., L.M., F.R., A.P., N.A., A.M.A., S.P., F.M., S.L., and L.C. analyzed data; and F.S. and L.C. wrote the paper.

The authors declare no competing interest.

1. S. Merrill, Keeping it real? Subcultural graffiti, street art, heritage and authenticity. *Int. J. Herit. Stud.* **21**, 369–389 (2015).
2. Banksy, Exit Through the Gift Shop. Producers Distribution Agency (sound film, Jaimie D'Cruz, United Kingdom, 2010).
3. P. Mezzadri, Contemporary murals in the street and urban art field: Critical reflections between preventive conservation and restoration of public art. *Heritage* **4**, 2515–2525 (2021).
4. L. Pagnin, N. Guarnieri, F. C. Izzo, S. Goidanich, L. Toniolo, Protecting street art from outdoor environmental threats: What are the challenges?. *Coatings* **13**, 2044 (2023).
5. I. M. Cortea, L. Ratoiu, R. Radvan, Characterization of spray paints used in street art graffiti by a non-destructive multi-analytical approach. *Color Res. Appl.* **46**, 183–194 (2021).
6. G. Germinario, I. D. van der Werf, L. Sabbatini, Chemical characterisation of spray paints by a multi-analytical (Py/GC–MS, FTIR, u-Raman) approach. *Microchem. J.* **124**, 929–939 (2016).
7. D. Cimino, R. Lamuraglia, I. Saccani, M. Berzioli, F. C. Izzo, Assessing the (in)stability of urban art paints: From real case studies to laboratory investigations of degradation processes and preservation possibilities. *Heritage* **5**, 581–609 (2022).

8. G. Pellis *et al.*, Multi-analytical approach for precise identification of alkyd spray paints and for a better understanding of their ageing behaviour in graffiti and urban artworks. *J. Anal. Appl. Pyrolysis* **165**, 105576 (2022).
9. V. Marazioti *et al.*, Facorellis chemical characterisation of artists'spray-paints: A diagnostic tool for urban art conservation. *Spectrochim. Acta A Mol. Biomol. Spectrosc.* **291**, 122375 (2023).
10. E. C. Rigante, C. D. Calvano, R. A. Picca, F. Modugno, T. R. Cataldi, An insight into spray paints for street art: Chemical characterization of two yellow varnishes by spectroscopic and MS-based spectrometric techniques. *Vacuum* **215**, 112350 (2023).
11. S. A. Connors-Rowe, H. R. Morris, P. M. Whitmore, Evaluation of appearance and fading of daylight fluorescent water colors. *J. Am. Inst. Conserv.* **44**, 75–94 (2005).
12. V. Pintus, S. Wei, M. Schreiner, UV ageing studies: Evaluation of lightfastness declarations of commercial acrylic paints. *Anal. Bioanal. Chem.* **402**, 1567–1584 (2012).
13. M. T. Doménech-Carbó *et al.*, Study of behaviour on simulated daylight ageing of artists' acrylic and poly(vinyl acetate) paint films. *Anal. Bioanal. Chem.* **399**, 2921–2937 (2011).
14. A. Ciccola *et al.*, Spectroscopy for contemporary art: Discovering the effect of synthetic organic pigments on UVB degradation of acrylic binder. *Polym. Degrad. Stab.* **159**, 224–228 (2019).
15. M. M. Di Crescenzo, E. Zendri, M. Sánchez-Pons, L. Fuster-López, D. J. Yusá-Marco, The use of waterborne paints in contemporary murals: Comparing the stability of vinyl, acrylic and styrene-acrylic formulations to outdoor weathering conditions. *Polym. Degrad. Stab.* **107**, 285–293 (2014).
16. L. Pagnin, R. Calvini, K. Sterflinger, F. C. Izzo, Data fusion approach to simultaneously evaluate the degradation process caused by ozone and humidity on modern paint materials. *Polymers* **14**, 1787 (2022).
17. J. S. Pozo-Antonio, T. Rivas, N. González, E. M. Alonso-Villar, Deterioration of graffiti spray paints applied on granite after a decade of natural environment. *Sci. Total Environ.* **826**, 154169 (2022).
18. J. La Nasa *et al.*, A chemical study of organic materials in three murals by Keith Haring: A comparison of painting techniques. *Microchem. J.* **124**, 940–948 (2016).
19. D. Magrini *et al.*, A multi-analytical approach for the characterization of wall painting materials on contemporary buildings. *Spectrochim. Acta. Part A Mol. Biomol. Spectrosc.* **173**, 39–45 (2017).
20. J. La Nasa *et al.*, 60 years of street art: A comparative study of the artists' materials through spectroscopic and mass spectrometric approaches. *J. Cult. Herit.* **48**, 129–140 (2021).
21. A. Bosi *et al.*, Street art graffiti: Discovering their composition and alteration by FTIR and micro-Raman spectroscopy. *Spectrochim. Acta. A Mol. Biomol. Spectrosc.* **225**, 117474 (2020).
22. T. Rivas, E. M. Alonso-Villar, J. S. Pozo-Antonio, Forms and factors of deterioration of urban art murals under humid temperate climate; Influence of environment and material properties. *Eur. Phys. J. Plus* **137**, 1257 (2022).
23. F. Sabatini *et al.*, Fluorescent paints in contemporary murals: A case study. *Heritage* **6**, 5689–5699 (2023).
24. F. Armetta *et al.*, Chemistry of street art: Neural network for the spectral analysis of berlin wall colors. *J. Am. Chem. Soc.* **146**, 35321–35328 (2024).
25. C. Cucci, *et al.*, The colors of Keith Haring: A spectroscopic study on the materials of the mural painting Tuttomondo and on reference contemporary outdoor paints. *Appl. Spectrosc.* **70**, 186–196 (2016).
26. A. Rousaki *et al.*, An in-and-out-the-lab raman spectroscopy study on street art murals from Reggio Emilia in Italy. *Eur. Phys. J. Plus* **137**, 252 (2022).
27. N. Guarnieri *et al.*, Rapid chromatic alteration of street art: Mechanisms of deterioration of the painting materials of the 20 years of Freedom and Democracy mural. *Dyes Pigments* **239**, 112733 (2025). 10.1016/j.dyepig.2025.112733.
28. R. Radpour, J. K. Delaney, I. Kakoulli, Acquisition of high spectral resolution diffuse reflectance image cubes (350–2500 nm) from archaeological wall paintings and other immovable heritage using a field-deployable spatial scanning reflectance spectrometry hyperspectral system. *Sensors* **22**, 1915 (2022).
29. H. Liang, Advances in multispectral and hyperspectral imaging for archaeology and art conservation. *Appl. Phys. A* **106**, 309–323 (2012).
30. C. Cucci *et al.*, Fifteenth century Florentine mural investigated in situ with VNIR hyperspectral imaging and NIR photography supports interpretation as a bloodletting scene. *Sci. Rep.* **14**, 11698 (2024).
31. B. Schmitt, Z. Souidi, F. Duquesnoy, F. V. Donzé, From RGB camera to hyperspectral imaging: A breakthrough in Neolithic rock painting analysis. *Heritage Sci.* **11**, 91 (2023).
32. S. Kogou *et al.*, From remote sensing and machine learning to the history of the Silk Road: Large scale material identification on wall paintings. *Sci. Rep.* **10**, 19312 (2020).
33. D. Kaimaris, Aerial remote sensing archaeology–a short review and applications. *Land* **13**, 997 (2024).
34. E. Adamopoulos, F. Rinaudo, UAS-based archaeological remote sensing: Review, meta-analysis and state-of-the-art. *Drones* **4**, 46 (2020).
35. W. Fremout, S. Saverwyns, Identification of synthetic organic pigments: The role of a comprehensive digital Raman spectral library. *J. Raman Spectrosc.* **43**, 1536–1544 (2012).
36. F. Rosi *et al.*, Unveiling the composition of historical plastics through non-invasive reflection FT-IR spectroscopy in the extended near-and mid-infrared spectral range. *Anal. Chim. Acta* **1169**, 338602 (2021).
37. F. Rosi, A. Daveri, P. Moretti, B. G. Brunetti, C. Miliani, Interpretation of mid and near-infrared reflection properties of synthetic polymer paints for the non-invasive assessment of binding media in twentieth-century pictorial artworks. *Microchem. J.* **124**, 898–908 (2016).
38. I. Bargagli *et al.*, Assessing mechanochemical properties of Acrylonitrile Butadiene Styrene (ABS) items in cultural heritage through a multimodal spectroscopic approach. *Appl. Spectrosc.* **78**, 00037028241267325 (2024).
39. L. Monico, F. Rosi, C. Miliani, A. Daveri, B. G. Brunetti, Non-invasive identification of metal-oxalate complexes on polychrome artwork surfaces by reflection mid-infrared spectroscopy. *Spectrochim. Acta. A Mol. Biomol. Spectrosc.* **116**, 270–280 (2013).
40. L. Rampazzi, Calcium oxalate films on works of art: A review. *J. Cult. Herit.* **40**, 195–214 (2019).
41. M. F. Silva, M. T. Doménech-Carbó, L. Fuster-López, M. F. Mecklenburg, S. Martin-Rey, Identification of additives in poly (vinylacetate) artist's paints using PY-GC-MS. *Anal. Bioanal. Chem.* **397**, 357–367 (2010).
42. T. Palomar *et al.*, Analysis of chromophores in stained-glass windows using visible hyperspectral imaging in-situ. *Spectrochim. Acta A Mol. Biomol. Spectrosc.* **223**, 117378 (2019).
43. T. E. Townsend, Discrimination of iron alteration minerals in visible and near-infrared reflectance data. *J. Geophys. Res. Solid Earth* **92**, 1441–1454 (1987).
44. F. Remondino, Heritage recording and 3D modeling with photogrammetry and 3D scanning. *Remote Sens.* **3**, 1104–1138 (2011).
45. A. Adami, I. Cerato, E. d'Annibale, E. Demetrescu, D. Ferdani, *Different Photogrammetric Approaches to 3D Survey of the Mausoleum of Romulus in Rome* R. Klein P. Santos Eds., (EUROGRAPHICS Workshop on Graphics and Cultural Heritage, 2014).
46. F. Carvajal-Ramírez, A. D. Navarro-Ortega, F. Agüera-Vega, P. Martínez-Carricondo, Unmanned aerial vehicle photogrammetry and 3D modeling applied to virtual reconstraction of an archaeological site in the bronze age. *Int. Arch. Photogramm. Remote Sens. Spatial Inf. Sci.* **15**, 279–284 (2019).
47. N. Abate *et al.*, Integrated close range remote sensing techniques for detecting, documenting, and interpreting lost medieval settlements under canopy: The case of Altanum (RC, Italy). *Land* **12**, 310 (2023). 10.3390/land12020310.
48. M. Anghelone, V. Stoytschew, D. Jembrih-Simbürger, M. Schreiner, Spectroscopic methods for the identification and photostability study of red synthetic organic pigments in alkyd and acrylic paints. *Microchem. J.* **139**, 155–163 (2018).
49. M. Krmpotić, D. Jembrih-Simbürger, Z. Siketić, M. Anghelone, I. B. Radović, Study of UV ageing effects in modern artists' paints with MeV-SIMS. *Polym. Degrad. Stab.* **195**, 109769 (2022).
50. Z. E. Papliaka, K. S. Andrikopoulos, E. A. Varella, Study of the stability of a series of synthetic colorants applied with styrene–acrylic copolymer, widely used in contemporary paintings, concerning the effects of accelerated ageing. *J. Cult. Herit.* **11**, 381–391 (2010).
51. U. I. Gaya, A. Abdul Halim, Heterogeneous photocatalytic degradation of organic contaminants over titanium dioxide: A review of fundamentals, progress and problems. *J. Photochem. Photobiol. C, Photochem. Rev.* **9**, 1–12 (2008).
52. T. Schmitt *et al.*, New insights into the deterioration of TiO_2 based oil paints: The effects of illumination conditions and surface interactions. *Heritage Sci.* **10**, 99 (2022).
53. B. A. Van Driel, P. J. Kooyman, K. J. Van den Berg, A. Schmidt-Ott, J. Dik, A quick assessment of the photocatalytic activity of TiO2 pigments–From lab to conservation studio!. *Microchem. J.* **126**, 162–171 (2016).
54. B. A. Van Driel *et al.*, Determination of early warning signs for photocatalytic degradation of titanium white oil paints by means of surface analysis. *Spectrochim. Acta A Mol. Biomol. Spectrosc.* **172**, 100–108 (2017).
55. F. Sabatini *et al.*, Data set supporting the publication: "Unveiling street art: a multimodal and multitechnique approach for analysing and mapping painting materials on large murals." Zenodo. https://doi.org/10.5281/zenodo.16738845. Deposited 5 August 2025.